Continuous Symmetry Measures. 5. The Classical Polyhedra

Mark Pinsky[†] and David Avnir*

Institute of Chemistry and The Lise Meitner Minerva Center for Computational Quantum Chemistry, The Hebrew University of Jerusalem, Jerusalem 91904, Israel

Received April 30, 1998

The continuous symmetry measures approach, designed to assess quantitatively the degree of any symmetry within any structure, is extended to the important class of the polyhedra. For this purpose, we developed a general methodology and a general computational tool, which identify the minimal distance of a given structure to a desired general shape with the same number of vertexes. Specifically, we employ this tool to evaluate quantitatively the degree of polyhedricity within distorted polyhedra, taking as examples the most central and abundant polyhedral structures in chemistry in general and in coordination chemistry in particular, namely the tetrahedron, the bipyramid, the octahedron, the cube, the icosahedron, and the dodecahedron. After describing the properties of the symmetry measurement tool, we show its application and versatility in a number of cases where the deviation from exact symmetry has been an issue, including *z*-axis Jahn−Teller type polyhedral distortions, tantalum hydride complexes, pentacoordinated zinc complexes, tetrahedral/octahedral Sn complexes, and icosahedrally distorted C_{60}-fullerene anions.

1. Background

We have been advancing the notion, from the conceptual level up to practical applications, that there are certain advantages in treating symmetry as a structural property of continuous nature.[1] Symmetry has traditionally functioned as a condensed language for the description and classification of molecular and supramolecular shapes and structures and as an identifier of both apparent and inherent correlations between structure and physical properties of matter. Our study of symmetry has been based on the thesis that perfect symmetry is rarely attainable in reality; much more often than not, molecules are *not* symmetric. To realize it, one has to refine the resolution of observation, spatial or temporal, up to the point where it becomes evident. Consider, for instance, the observation of "symmetric" molecules on time scales that are faster then typical vibrations or rotation rates, or consider the local distortive forces on "symmetric" molecules in the condensed phase. Symmetry has served as an approximate, idealized descriptive language of this reality, and while it is true that an imprecise language helps in grasping complex situations and in identifying first-order trends, the danger of missing important intricate details of the complexity by this practice is there.

A natural approach to the treatment of the imprecise nature of symmetry is to allow flexibility in its description, namely, as mentioned above, to treat it as a structural property of *continuous* nature, complementary to the classical discrete point of view, as indeed proposed by several research groups.[2] A list of stringent demands must be fulfilled by any proposed continuos symmetry scale. Among these demands are the ability to express quantitatively how much of a given symmetry there is in any (distorted) structure, at any temporal resolution, at any spatial resolution, and with respect to any ideal element or group symmetry, the ability to express the distortion with a *single* parameter, the ability to compare all symmetries on the same scale, and the freedom from the need to select an arbitrary reference structure. The solution to the symmetry measurement problem, which we have proposed in a series of papers since 1992,[3] was shown to fulfill these requirements. It has proven to be general and practical and has passed the critical test of identifying quantitative correlations between the degree of symmetry and molecular properties in a wide variety of systems, examples of which are collected in ref 4. Furthermore, it has also passed the test that in our view is the most crucial one, namely, that in all of these studied cases, the identified correlations between property and symmetry translate correctly the physical qualitative intuition that one may have a priori on the existence and direction of such correlations.

In this report, we extend our methodology to the family of the high symmetries of the classical, perfect polyhedra,[5] the

* To whom correspondence should be addressed. E-mail: david@chem.ch.huji.ac.il (for part 4, see ref 9b).

[†] Also at the Institute of Earth Sciences, The Hebrew University of Jerusalem.

(1) Reviews: (a) Avnir, D.; Katzenelson, O.; Keinan, S.; Pinsky, M.; Pinto, Y.; Salomon, Y.; Zabrodsky Hel-Or, H. In *Concepts in Chemistry*; Rouvray, D. H., Ed.; Research Studies Press: Somerset, 1997; Chapter 9. (b) Avnir, D.; Zabrodsky Hel-Or, H.; Mezey, P. G. In *Encyclopedia of Computational Chemistry*; von Rauge Schleyer, P., Ed.; Wiley: Chichester, in press.

(2) Some examples for symmetry measurements (see also citations in ref 1): (a) Maaskant, W. J. A. *J. Phys.: Condens. Matter* **1997**, *9*, 9759. (b) Zimpel, Z. *J. Math. Chem.* **1993**, *14*, 451. (c) Auf der Heyde, T. P. E.; Bürgi, H.-B. *Inorg. Chem.* **1989**, *28*, 3960. (d) Murray-Rust, P.; Bürgi, H. B.; Dunitz, J. D. *Acta Crystallogr.* **1978**, *B34*, 1787. The problematics of selecting a specific reference structure was discussed in another paper by these authors: Murray-Rust, P.; Burgi, H.-B.; Dunitz, J. D. *Acta Crystallogr.* **1979**, *A35*, 703. (e) Cammi, B.; Cavalli, E. *Acta Crystallogr.* **1992**, *B48*, 245. Cavalli, E.; Cammi, R. *Comput. Chem.* **1994**, *18*, 405. (f) Mezey, P. G. In *Fuzzy Logic in Chemistry*; Rouvray, D. H., Ed.; Academic Press: San Diego, 1997; pp 139. (g) Korobko, V. I. *Symmetry: Culture and Sci*. **1995**, *6*, 308. (h) Klein, D. J. *J. Math. Chem.* **1995**, *18*, 321. (i) Kuz'min, V. E.; Stel'mach, I. B.; Bekker, M. B.; Pozigun, D. V. *J. Phys. Org. Chem.* **1992**, *5*, 295. (j) Toporova, A. P.; Toporov, A. A.; Ishankhodzhaeva, M. M.; Parpirev, N. A. *Russ. J. Org. Chem.* **1996**, *41*, 466. (k) Grunbaum, B. *Proc. Symp. Pure Math.: Am. Math. Soc.* **1963**, *7*, 233.

(3) (a) Zabrodsky Hel-Or, H.; Peleg, S.; Avnir, D. *J. Am. Chem. Soc.* **1992**, *114*, 7843. (b) Zabrodsky Hel-Or, H.; Peleg, S.; Avnir, D. *J. Am. Chem. Soc.* **1993**, *115*, 8278.

10.1021/ic9804925 CCC: $15.00
Published on Web 10/02/1998

regular, Platonic polyhedra, namely, the tetrahedron, the octahedron, the cube, the icosahedron, and the dodecahedron, as well as to the D_{nh} equilateral bipyramids, taking the trigonal bipyramid as a case example. These polyhedra represent also the prism (cube) and antiprism (octahedron) polyhedra families.[5] The role that these structures play in chemistry and in particular in coordination chemistry is so central[6] that only with this report we feel that we begin to approach completion of the continuous symmetry measures (CSM) methodology as a general working tool.

The development described here provides a practical and convenient way of answering questions such as "how much octahedricity is there in a distorted octahedron?"; "which in a set of icosahedral fullerenes is the most distorted one?"; "what is the degree of a Jahn−Teller degeneracy removal distortion?"; "by how much does the symmetry of a fluxional bipyramid change along the isomerization mode?"; and so on. We investigate currently several of these key questions; at the moment we devote this report to the methodology itself, its underlying base, its properties, and its application to some real data.

2. Continuous Symmetry Measure

The design of a measurement tool, which translates the concept of continuous symmetry into practice, involves a certain degree of arbitrariness, in the sense that one has to decide on issues such as how should the zero-reference level be set, what should be the maximal value, what should be the actual measurement yardstick, what normalization procedures should one employ, and so on. Having this in mind, we set up to base the symmetry measure on a definition that would be as minimalistic as possible.[3a] The amount of a given symmetry in a structure is a function of the minimal distance that the vertexes of the structure have to undergo in order for it to attain the desired symmetry. In a more formal way, the continuous symmetry measure (CSM) of the original structure is a normalized root-mean-square deviation from the closest structure with the desired symmetry. It is a distance function the end point of which is being searched. We emphasize the generality of this definition. It does not seek the distance to a preset reference structure;[2d,e] but to a required symmetry. Thus, given a (distorted) structure composed of N vertexes, the coordinates of which are given by the vector $\{Q_k, k = 1, 2, ..., N\}$, we search for the vertex coordinates $\{\hat{P}_k, k = 1, 2, ..., N\}$ of the nearest perfectly G-symmetric object (G being a specific symmetry group) and define the symmetry measure as

$$S = \min \frac{\sum_{k=1}^{N} |Q_k - P_k|^2}{\sum_{k=1}^{N} |Q_k - Q_0|^2} \times 100 \qquad (1)$$

Here Q_0 is the coordinate vector of the center of mass of the investigated structure

$$Q_0 = \frac{1}{N} \sum_{k=1}^{N} Q_k \qquad (2)$$

The CSM defined in (1) is independent of the position, orientation, and size of the original structure. Equation 1 is general and allows one to evaluate the symmetry measure of *any* shape relative to *any* symmetry group G or element. $|Q - P|^2$ is a "measure" (a metric), the units of which are length squared. To avoid size effects, the size of the original structure is normalized to the rms distance from the center of mass of the structure (placed at the origin) to all vertexes. As proven below, the bounds are $100 \geq S \geq 0$. However, since the practice in symmetry-related studies has been to focus on small distortions, we found it convenient to expand the 0−1 range by a factor of 100. If a structure has the desired G-symmetry, $S(G) = 0$. The symmetry measure increases as it departs from G-symmetry and reaches a maximal value (not necessarily 100).[3b] All $S(G)$ values, regardless of G, are on the same scale and are therefore comparable; one can compare the degree of, say, octahedricity of various distorted octahedral complexes, the symmetry content of various symmetry subgroups in one octahedron (C_3-ness, C_{3v}-ness, etc.), and even different symmetries in different objects.

Since the use of similarity or distance functions as structural descriptors is a known approach,[7] it is in order to reiterate a unique aspect of eq 1, mentioned briefly above. A standard approach has been to define a *specific (ideal) reference structure*, identified through a specific set of (Cartesian or symmetry[2]) coordinates and to find the distance of the studied structure from this preset reference. A more general and demanding task, adapted by the CSM approach, has been to *find* the coordinates of the nearest ideal reference structure (the perfectly symmetric one).[2d] For example, if one wishes to determine the degree of C_{3v}-ness in a tetrahedron, the nearest C_{3v} structure out of an infinite library is searched, located, and displayed.[3b,8]

3. Polyhedral CSM Approach: The Distance to a Shape

The main practical problem is then how to find the nearest structure that has the desired symmetry, namely how to locate the specific set of $\hat{P}$'s that minimizes eq 1. In a series of papers, a detailed solution to that problem was provided, which is based on what we termed the "folding−unfolding" algorithms. It is a general approach, which analyzes *all* of the elements that comprise a given symmetry point group (see detailed description in refs 3 and 9). We found, however, that the large number of symmetry elements of the perfect polyhedra renders the folding−unfolding approach cumbersome beyond the tetrahedron.[3b] As a consequence and without giving away any of the generality and restrictions imposed by the definition of the CSM (eq 1), we developed and present here a different approach that allows one to evaluate the degree of perfect polyhedral symmetry in

(4) Examples include the following. (a) Application of centrosymmetry measure as an order parameter in the study of the melting point of icosahedral clusters: Buch, V.; Greshgoren, E.; Zabrodsky Hel-Or, H.; Avnir, D. *Chem. Phys. Lett.* **1995**, *247*, 149. (b) Quantitative investigation of the chirality properties of the cyclic trimer of water and of its enantiomerization pathways: Pinto, Y.; Zabrodsky Hel-Or, H.; Avnir, D. *J. Chem. Soc., Faraday Trans.* **1996**, *92*, 2523. (c) Analysis of the correlation between the degree of centrosymmetry and hyperpolarizability: Kanis, K. D.; Wong, J. C.; Marks, T. S.; Ratner, M. A.; Zabrodsky, H.; Keinan, S.; Avnir, D. *J. Phys. Chem.* **1995**, *99*, 11061. (d) Quantitative analysis of the chirality of large random objects: Katzenelson, O.; Zabrodsky Hel-Or, H.; Avnir, D. *Chem. Eur. J.* **1996**, *2*, 174. Avnir, D.; Katzenelson, O.; Zabrodsky Hel-Or, H. *Chem. Eur. J.* **1996**, *2*, 744. (e) Analysis of the macroscopic chirality of Pasteur's tartrate crystals: Keinan, S.; Zabrodsky Hel-Or, H.; Avnir, D. *Enantiomer* **1996**, *1*, 351 and refs 21 and 22 below.

(5) Hargittai, I.; Hargittai, M. *Symmetry through the eyes of a chemist*, 2nd ed.: Plenum Press: N.Y., 1995.

(6) Muller, U. *Inorganic Structural Chemistry*, 2nd ed.; Wiley & Sons: Chichester, 1992.

(7) Rouvray, D. H. *Top. Curr. Chem.* **1995**, *173*, 1. Petitjean, M. *J. Chem. Inf. Comput. Sci.* **1996**, *36*, 1038.

classical (distorted) polyhedra, overcoming the difficulty of many elements in a group. As mentioned above, these include as examples (but are not limited to) the regular polyhedra (tetrahedron, octahedron, cube, icosahedron, and dodecahedron) and the bipyramids.

The solution is general from a point of view not shared with the folding−unfolding algorithms; it allows one to determine the distance from any required shape ("shape" and not "structure": the latter is a specific reference with specific coordinates, while the former does not specify size, orientation, etc). The target shape may be of polyhedral symmetry, of lower symmetry, or even distorted with no symmetry. Here we concentrate on the perfect polyhedral shapes, but practically all of the considerations and results detailed below are applicable to any other target shape. (Application of this general solution to other shapes and symmetries is planned for subsequent reports.) Thus, since the general shape of a polyhedron is a readily attainable information input, the complex case of evaluating the degree of prefect polyhedricity is simplified; it is reduced to the search of the size and orientation of the perfectly symmetric target. Let us then describe the methodology.

Given a distorted polyhedron with N vertexes, the coordinates of which are given by the vector $\{Q_k, k = 1, 2, ..., N\}$ (Figure 1a), we search for the vertex coordinates $\{\hat{P}_k, k = 1, 2, ..., N\}$ of the nearest perfectly symmetric polyhedron (Figure 1b), as defined above through eq 1. By perfectly symmetric we mean here the highest possible symmetry group (e.g., T_d for a four-vertex configuration). For all polyhedra taken as examples here, except the trigonal bipyramid, this also means equal distance from the center of mass to all vertexes. This, however, is not an intrinsic requirement in the methodology; the ideal trigonal bipyramid we selected is of equal faces, and this dictates unequal distances from the center of mass to the vertexes (which, nevertheless, are simply interrelated). By distorted we mean polyhedra that are of symmetry lower than that highest (say, a C_3-tetrahedron and, obviously, a C_1 polyhedron and so on). To be useful for analysis of complexes, the central atom is included, if desired, as well (Figure 1c,d). No connectivity is assumed here; the connectivity displayed in Figure 1 serves only for graphical convenience. The polyhedral CSM is determined by the following multiple minimizations procedure.

1. The coordinates of the center of mass of the nonsymmetric N-polyhedron (for example, a distorted octahedron, Figure 1a) are calculated, and the polyhedron is placed at the origin of Cartesian coordinates, i.e., at $Q_0 = 0$ (eq 2). The orientation and size are either arbitrary or selected for convenience of computation.

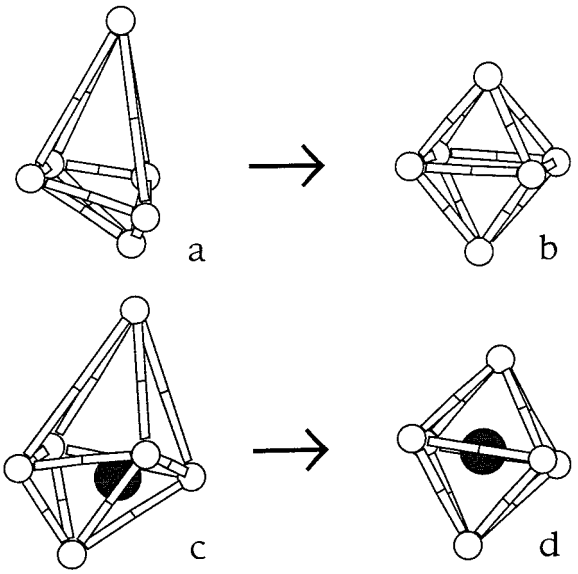

Figure 1. Polyhedral symmetry measures approach evaluates the degree of symmetry content in distorted polyhedra. For instance, here we evaluate the degree of octahedricity of the distorted octahedron, **a**. The approach is to search for the nearest structure with the desired symmetry, **b**, identify it, and calculate the distance to it using eq 5. From this equation, the degree of octahedricity of **a** is $S(O_h) = 14.95$. Symmetry analyses can also be carried out with the inclusion of the central atom, as in **c** (the distorted one), leading to **d** (the nearest symmetric one). This example was selected too to give $S(O_h) = 14.95$ as well (cf., caption of Figure 2).

2. The target shape, a perfect N-polyhedron of size 1 (a perfect octahedron, in our example), is also placed at $Q_0 = 0$ with an arbitrary orientation and with arbitrary vertex labeling, $\{P_{0k}, k = 1, 2, ..., N\}$. This defines the searched general *shape*. This preliminary prototype structure is *not* of minimal distance from the nonsymmetric structure. It defines the desired shape and serves as a starting point for the minimization search procedure.

3. The transformation that the set P_{0k} has to undergo to yield the desired set of $\hat{P}_k$, namely the set which is closest to Q_k, is now to be determined. This means that one should determine the isotropic scaling factor, A, the rotation (3×3) matrix, $\mathbf{R}$, and the displacement (3×1) vector, $\mathbf{T}$, all for the desired transformation of P_{0k}:

$$P_k = A\mathbf{R}P_{0k} + \mathbf{T} \tag{3}$$

It follows that finding a symmetric polyhedron that will be the most similar (in the root-mean-square sense) to the starting polyhedron amounts to obtaining A, $\mathbf{R}$, and $\mathbf{T}$ from the minimization of the sum function

$$J = \sum_{k=1}^{N} |Q_k - P_k|^2 = \sum_{k=1}^{N} |Q_k - (A\mathbf{R}P_{0k} + \mathbf{T})|^2 \tag{4}$$

Several minimizations are involved here. In Appendix A we detail the derivations and technical details involved in these minimizations, which are the following ones.

4. Minimization of $\mathbf{T}$ leads to $\mathbf{T} = 0$ (Appendix A), i.e., the selection to place the two polyhedra at the same origin (step 2) renders this minimization unnecessary. The result $\mathbf{T} = 0$ means

(8) The term "continuous" is used here in contradistinction to "either/or". It is a general term that has been used with various connotations. For instance, in physics, continuous symmetry means that by performing a continuous transformation of a set of parameters on a physical system it acts the same way everywhere and at all times (Gross, D. J. *Proc. Natl. Acad. Sci. U.S.A.* **1993**, *93*, 14256). Lie groups used for gauge symmetries are another place where this term is used, especially in the context of invariance to continuous changes in the coordinates of observation (Rosen, J. *Found. Phys*. **1990**, *20*, 283. Pons, J. M. *Mod. Phys. Lett*. **1994**, *9*, 2903). Of relevance are also several studies in spectroscopy. Thus, continuity was suggested for asymmetric rotors (King, G. W.; Heiner, R. M.; Cross, P. C. *J. Phys. Chem*. **1942**, *11*, 27), although the parameter developed there does not measure the distance from specific symmetries. Near-symmetry has been also treated in spectroscopy in terms of perturbation theory: Bunker, P. R. *Molecular Symmetry and Spectroscopy*; Academic Press: New York, 1979; Chapter 11. Symmetry of nonrigid molecules was treated in the following: Longuet-Higgins, H. C. *Mol. Phys*. **1967**, *6*, 445. Louk, J. D.; Galbreith, H. W. *Rev. Mod. Phys*. **1976**, *48*, 69. The latter reference was through the use of Eckart vectors. Yet another worth noting approach to the expression of structural deviation is the use of matrix elements, which are a power-series expansion in normal modes displacements: Frey, R. F.; Davidson, E. R. *J. Chem. Phys*. **1988**, *88*, 1775. See also refs 2d and e.

(9) (a) Zabrodsky Hel-Or, H.; Peleg, S.; Avnir, D. *Adv. Mol. Struct. Res.* **1995**, *1*, 1. (b) Zabrodsky Hel-Or, H.; Peleg, S.; Avnir, D. *J. Am. Chem. Soc*. **1995**, *117*, 462.

also that the centers of mass do not move from the origin following this minimization search.

5. The spatial mutual orientation of the two structures is minimized. This is done by determination of the elements of the rotation matrix **R** that yield the minimal *J*.

6. The size difference between the polyhedra is minimized by determination of the isotropic scaling factor, *A*. Together with the minimization of step 5, this leads to best overlap of the two polyhedra. These two minimizations can be carried out in reverse order without affecting the outcome (see Appendix A).

7. The next minimization is over the labeling of the vertexes, i.e., minimizations 5 and 6 are repeated over all possible corresponding pairings between the vertexes of the prototype and nonsymmetric polyhedra in order to locate the set of $\{Q_k \sim P_j,\ k, j = 1, 2, ..., N\}$ that minimizes *J* (eq 4). The total number of repetitions equals *N*!. In most cases, the correspondence of vertexes of the prototype and nonsymmetric polyhedra can be specified a priori, and then minimization 7 is not needed. In fact, for polyhedra that exceed eight to nine vertexes, prepairing is desirable in order to save on computing time which grows as *N*!.

8. As detailed in Appendix A, these minimizations lead to

$$S = \left[1 - \frac{(\sum_{k=1}^{N} P_{0k}^{t}\mathbf{R}^{t}Q_k)^2}{N\sum_{k=1}^{N}|Q_k|^2}\right] \times 100 \qquad (5)$$

where the upper index, t, shows the transposition of the matrix or vector. The minimal *S* is calculated from eq 5. Using $\hat{P}_k = A\mathbf{R}P_{0k}$, one obtains the structure of the nearest symmetric polyhedron (Figure 1b). Like the parent eq 1, eq 5 is also bound within the interval $100 \geq S \geq 0$;[10] the symmetry measure attains its minimum value ($S = 0$) when the structure has the desired symmetry. In this case $P_{0i}^{t}\mathbf{R}^{t}Q_i = |Q_i| = Q = \text{const}$ so that the ratio in square brackets in eq 5 is equal to 1. The maximal value of 100 is obtained for cases where the nearest object with the desired symmetry is the center point. (An example would be the degree of hexagonality of a pentagon; the nearest hexagon to a pentagon is that center point, and because of the size normalization, the distance to it is 1×100.) Otherwise its upper limit is less than 100 and depends on the polyhedron type and on the specific structure that is analyzed, as shown in the next section.

We conclude this section with a few comments:

i. In symmetry analyses of polyhedral coordination complexes it is often of relevance and of interest to include also the central atom. The procedure for such cases follows the same eight steps, and parts c and d of Figure 1 exemplify it. Note that the center of mass (step 1) need not coincide with the central atom in the distorted polyhedron (Figure 1c) but must coincide with it in the nearest symmetric one (Figure 1d).

ii. Earlier, we proved that the folding−unfolding algorithm leads to the minimal *S* value;[3,8] here the minimization is the procedure itself.[11]

iii. It is clear now that this method and its resulting eq 5 are a general solution to the problem of finding the minimal distance from any shape. It applies to all cases where the general shape of the desired nearest structure is known but not its size and orientation.

iv. In Appendix B, we derive an important result, linking the continuous symmetry measure with the correlation coefficient probability measure. We show there that given a random set of points, its *S* value with respect to the nearest symmetric polyhedron is given by

$$S = (1 - \rho^2) \times 100 \qquad (5')$$

where ρ is the sampling correlation coefficient between the original coordinates of the random points and the vertex coordinates of the nearest symmetric polyhedron. In other words, the minimization procedure for obtaining *S* can be interpreted as a least-squares procedure for obtaining information on an ordered structure (the perfect symmetric polyhedron) from the given random points set. Again, the result (eq 5′) is general and holds not only for the polyhedra but also for all cases where a target shape is specified.

4. Properties of the Polyhedral Symmetry Measure and Examples of Applications

I. Isosymmetry. The versatility of the measurement tool and its application are first demonstrated in Figure 2 for a variety of model polyhedra with a central atom, including a tetrahedron, an equilateral trigonal bipyramid, a cube, an icosahedron, and a dodecahedron. The nearest symmetric polyhedra are shown as well. The specific set of distorted polyhedra in Figures 1 and 2 was set up to give $S = 14.95$ for all polyhedra. We term structures having the same *S* value *isosymmetric.* Structures that are isosymmetric deviate from their specific selected perfect symmetry to the same degree. The CSM approach allows symmetry content comparison both between various distortions of the same polyhedron or between different polyhedra (see next example).

II. *z*-Axis Jahn−Teller Type Symmetry-Reducing Motions in Model Polyhedra. Jahn−Teller (JT) effects are a major cause of molecular symmetry reduction in general and symmetry reduction of polyhedral transition complexes in particular.[5,6] A common distortive mode, for instance in octahedral copper complexes, is the E_g elongation and compression along the *z*-axis (the Q_θ mode[12a]), reducing the symmetry from O_h to D_{4h}.[12] It is a central theme in our approach to propose that rather than discussing the JT effect in terms of jumps from one symmetry to another, it is more natural to attach a scale to this effect in terms of the residual content of the higher symmetry. Thus, a small JT effect in a copper complex means a small $S(O_h)$ value, and larger JT distortions are manifested by larger *S* values. In principle, the way is then open to link

(10) This is also a direct outcome from the Caushi−Bunykovsky inequality (Korn, G. A.; Korn, T. M. *Mathematical Handbook for Scientists and Engineers*; McGraw-Hill: New York, 1968; p 831).

$$N\sum_{k=1}^{N} c_k^{\,2} \geq (\sum_{k=1}^{N} c_k)^2$$

Using this inequality and definition of the vector P_{0k}, one obtains

$$N\sum_{k=1}^{N}|Q_k|^2 \geq N\sum_{k=1}^{N}(P_{0k}^{t}R^{t}Q_k)^2 \geq (\sum_{k=1}^{N}P_{0k}^{t}\mathbf{R}^{t}Q_k)^2 \geq 0$$

and from it the bounds of *S*.

(11) Consequently, the two methods should lead to the same results. Tests were carried out to compare the outcome of the folding−unfolding tetrahedron algorithm[3b] (the only perfect polyhedral program we developed by that method) with the results of the algorithm described here, and as should be the case, the two resulting *S* values are indeed the same.

(12) (a) Comba, P.; Zimmer, P. *Inorg. Chem.* **1994**, *33*, 5368. (b) Chapter 6.6 in ref 5 and references therein.

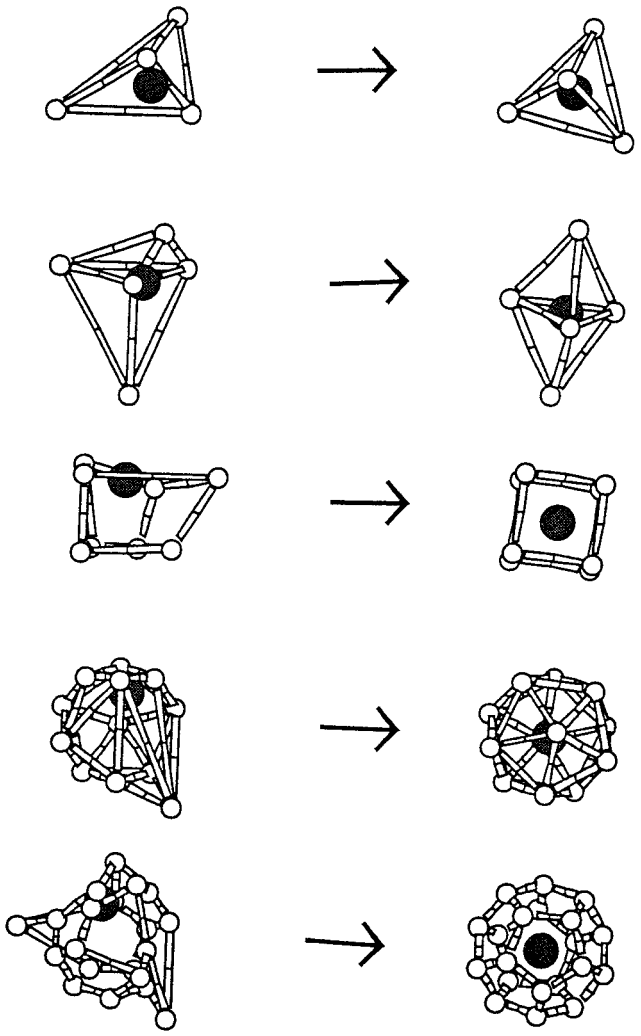

Figure 2. Versatility of the polyhedral symmetry measure, demonstrated (from top to bottom) for a tetrahedron, an equilateral trigonal bipyramid, a cube, an icosahedron, and a dodecahedron, all distorted and all with a misplaced central atom. The nearest perfect polyhedra, identified by the computational tool, are shown as well. All of the distorted polyhedra (and the octahedra of Figure 1) have the same *S* value of 14.95; i.e., their distances from their respective polyhedricities are equal. Thus, all of the distorted polyhedra are *isochiral*.

quantitatively the level of spectral splitting to the degree of symmetry distortion. It is a very important issue that deserves an in-depth separate report. Our aim in this introductory paper is the development of the appropriate tool and the analysis of its properties. What we do then in this subsection is to show that the polyhedral symmetry measure is also well behaved in responding to gradual continuous changes in structure, of relevance to the JT effect.

Figure 3 follows the $S(G)$ changes of a trigonal bipyramid, an octahedron, and an icosahedron, all without a central atom and all deformed along the *z*-axis. The "deformation ratio" is the ratio of the distances between the *z*-axis vertexes in the distorted and the symmetric polyhedra. Figure 3 shows the whole picture up to the limits. Severely distorted polyhedra can be found in small clusters at elevated temperatures[13] and along the pathway of the isomerization of fluxional complexes.[14] Let us analyze Figure 3. As should be the case, when the

(13) (a) Stillinger, F. H.; Weber, T. A. *J. Chem. Phys.* **1984**, *81*, 5095. (b) Wales, D. J.; Berry, R. S. *Phys. Rev. Lett.* **1994**, *73*, 2857.
(14) Sokolov, V. I. *Introduction to Theoretical Stereochemistry*; Gordon and Breach, New York, 1991; Chapter 4.

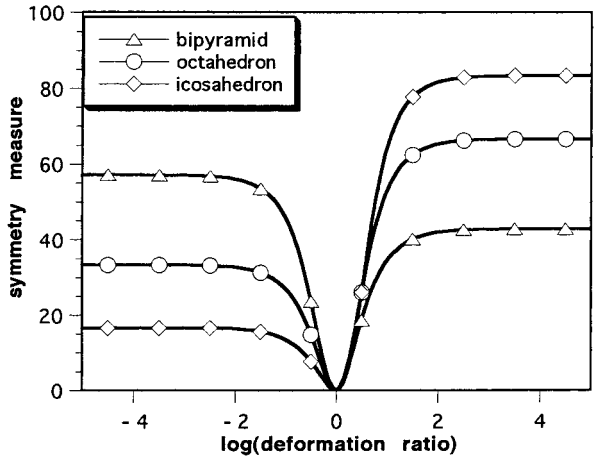

Figure 3. Symmetry measure values, $S(G)$, as a function of the deformation ratio for a trigonal bipyramid, an octahedron, and an icosahedron, all without a central atom and all deformed along the *z*-axis (i.e., the axis passing through the top and bottom vertexes of the symmetric trigonal bipyramid shown in Figure 2, through these vertexes in the octahedron **b** of Figure 1, and through any opposite vertexes in the symmetric icosahedron).

deformation ratio equals 1, the *S* values for the three polyhedra are zero. Recalling that the *S* scale is global so that it is possible to compare the symmetry content of deformed polyhedra with different numbers of vertexes, it is seen that the three polyhedra have different symmetry sensitivities to the same distortion parameter value and to its direction. Compression, left to the minimum, affects the bipyramid more than the octahedron and more than the icosahedron. On the other hand, the order of sensitivity of elongation, right to the minimum, reverses, icosahedron > octahedron > bipyramid. These different orderings can be understood by considering the two different limiting structures for the polyhedra; for elongation, it is a straight line onto which all vertexes have coalesced, and for the compression, it is a planar structure that contains all vertexes. We have seen that the rate of approaching these structures depends on the number of vertexes. Let us then consider a polyhedron that approaches a sphere. For a sphere, the average distance of a surface point to the diameter line is larger than the distance to the intersecting circle that contains it. Therefore, the effort (per vertex) to reach the nearest line increases with the number of vertexes, while the effort to reach the nearest plane, decreases. Finally, the limiting *S* values of the various polyhedra (Figure 3) are easily calculated from their geometrical properties and from eq 5. For instance, for the octahedron the limits are $(2/3) \times 100$ for infinite elongation and $(1/3) \times 100$ for compression; see Appendix C for details.

The arguments for the relative ordering in Figure 3 hold for the larger distortions. In fact, the picture is more complex, because the smaller deformations behave differently. Figure 4a shows a detail of Figure 3, namely mild deformations of up to 10%, as is commonly encountered in JT distorted molecules and in many other coordination compounds. As seen in Figure 4a, close to the minimum, the same ordering is kept on both sides, and the reversal of the ordering occurs only when elongation becomes more pronounced (Figure 4b). Note that the points of lines-crossings in Figure 4b are isosymmetric; the two polyhedra with the same deformation ratio differ from ideality at that point, to the same extent. Isosymmetry does not need, however, the same deformation ratio. Pass a horizontal line in any part of Figures 3 or 4; then all points of intersection with that line have the same *S* value and are

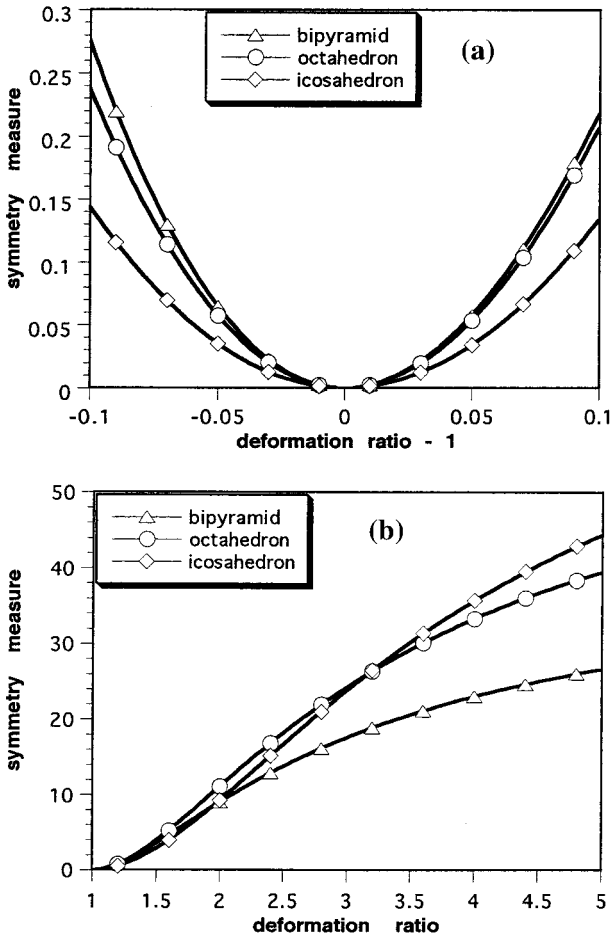

Figure 4. Details of Figure 3: (a) mild deformation levels (deformation ratio −1 is used here for clarity); (b) crossing points of the symmetry/deformation-ratio lines.

therefore isosymmetric, i.e., all, whether the same polyhedra or different ones, deviate similarly from perfect polyhedricity.

III. Tantalum Hydride Complexes. It is important to demonstrate that the polyhedral CSM approach is a working tool on real molecules beyond models, so these will be the next four cases of this section. For this purpose, we selected some cases from the published literature where distortion of symmetry has been a noticeable observation or a main issue. We begin with the report of Visciglio et al.[15] who studied the structure of six-coordinated tantalum dihydrides as part of ongoing research on the mechanism of the catalytic activity of transition metal hydrides. Catalytic activity is often highly sensitive to the intricate details of structure, and so in particular these authors reported that the analysis of the solid-state structure of $Ta(H)_2$-$(OC_6H_3Pr^i_2\text{-}2,6)_3(PMe_2Ph)$ revealed this complex to be "severely distorted from octahedral". The point we wish to make here is simple—the CSM methodology allows one to quantify this type of statement, which abounds in the literature, into a quantitative one; the degree of octahedricity, $S(O_h)$, of this complex is 4.37. Beyond quantification of statements of distortion, scaling the degree of symmetry opens the possibility to look for quantitative correlations between properties, say catalytic activity in this example and symmetry (see below).

IV. Pentacoordinated Zinc. The previous case was described as "severely distorted".[15] To build a bridge between the routine qualitative language of crystallographers and the symmetry scale, let us take now a case that is described as "slightly distorted". It is the pentacoordinated Zn trigonal bipyramid, $[Zn(II)]_2$(diacetoamido-glutarate)-hexaaquo·$2H_2O$, studied by Gomez-Lara et al.[16] in the context of the interaction of transition metal ions with *N*-acetylated groups in proteins. The coordination is to oxygen atoms, two of the glutarate and three of the water molecules. Another feature of the CSM approach is that while details for this complex are given in a lengthy table (Table 3 in ref 16), as is the routine practice, the methodology presented here allows a significant condensation in grasping the deviation, from a table full of data to a single value, which in this case is $S(D_{3h}$-equilateral$) = 1.48$. It is in order to recall here that *S* is a global value from which specific structural details cannot be extracted back. This globality is both the weakness and the strength of that approach, as with any thermodynamic function. Thus, the strength here is that the $S(O_h) = 4.37$ of the previous tantalum complex and the $S(D_{3h}) = 1.48$ are on the same scale and can be compared. As a result of space limitation, we are not reproducing the original tables and figures of these two complexes, but the interested reader who wishes to see what is meant by "severely distorted" and by "slightly distorted" may wish to compare Figure 2 in ref 15 and Figure 1 in ref 16.

Finally, we use this Zn complex study in order to comment on the limits of sensitivity of the CSM measurement tool. The Zn complex crystallized in fact as a dimer of two complexes; one has an *S* value of 1.4776 and the other 1.4687. Because of its importance, we devote a separate report to the issue of evaluating of errors in *S*(G) and assessing the probability that a given symmetry can be assigned to a (distorted) structure, on the basis of the uncertainty in the X-ray data (cf. also ref 9a).

V. Which Symmetry Represents Better a Given Complex? The "either/or" attitude toward symmetry labeling leads often to a "conflict of identity", in particular in cases where the structure shows characteristics of two different polyhedra, either because it seems to be similarly distorted with respect to the two options or because it is relevant to count all or only part of the ligand bonds.[17] One finds in such reports lengthy discussions on whether the structure is that of polyhedron A or of polyhedron B. The CSM approach addresses this conflict in a natural way; it characterizes the structure in terms of the degree of polyhedricity A as well as the degree of polyhedricity B, two values that are on the same scale. Unclear polyhedral identity characterizes, for instance, some tin complexes where, depending on how many of the differently attached ligands are counted, the complex may be regarded as either a tetrahedron or a trigonal bipyramid,[17] or as either a tetrahedron or an octahedron.[18] The latter case was addressed recently by Cea-Oliveras et al.[18] who have prepared SnS_6 complexes where four sulfur atoms are coordinated directly and two additional sulfur atoms, which are located within octane rings, interact transannularly with the central Sn (see Figure 1 in ref 18). Thus, a main discussion point in that study were structures that "can best be described as intermediate between tetrahedral and octahedral", concluding for the SnS_6 structures that the "possible relation with an octahedral geometry is less obvious".[18] By the CSM approach, the SnS_6 structure has an $S(O_h)$ value of 8.11. As for the SnS_4, our methodology actually allows one to carry

(15) Visciglio, V. M.; Fanwick, P. E.; Rothwell, I. P. *J. Chem. Soc., Chem. Commun.* **1992**, 1505. Here and below, coordinates are available on the PDB.

(16) Gomez-Lara, J.; Toscano, R. A.; Negron, G.; Zarate, E.; Campero, A. *J. Chem. Crystallogr.* **1994**, *24*, 441.

(17) For example: Swisher, R. G.; Holmes, R. R. *Organometallics* **1984**, *3*, 365.

(18) Cea-Oliveras, R.; Lomeli, V.; Hernandez-Ortega, S.; Haiduc, I. *Polyhedron* **1995**, *14*, 747.

Table 1. Degree of the Octahedricity and of All Possible Tetrahedricities of S_nS_6[18]

	symmetry measures		atom nos.[a]						
struct	G	*S*(G)	1	2	3	4	5	6	7
1	O_h	8.11	*	*	*	*	*	*	*
2	T_d	27.41	*	*			*	*	*
3	T_d	14.12	*	*	*		*		*
4	T_d	14.85	*	*		*	*		*
5	T_d	7.14	*	*	*			*	*
6	T_d	17.18	*	*		*		*	*
7	T_d	19.88	*	*	*	*			*
8	T_d	13.71		*	*		*	*	*
9	T_d	13.51		*		*	*	*	*
10	T_d	32.27		*	*	*	*		*
11	T_d	16.75		*	*	*		*	*
12	T_d	16.97	*		*		*	*	*
13	T_d	6.81	*			*	*	*	*
14	T_d	16.29	*		*	*	*		*
15	T_d	0.95	*		*	*		*	*
16	T_d	17.92			*	*	*	*	*

[a] Numbering of the sulfur atoms:

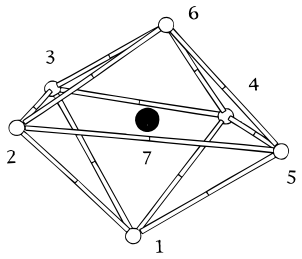

a blind search over all S_4 combinations out of the S_6 ligands, looking for the *minimal* $S(T_d)$ value. When one does so (Table 1), one obtains that the best tetrahedron has an $S(T_d)$ value of 0.95, significantly lower than the octahedricity value. The tin complex is much better described as a (slightly distorted) tetrahedron than an octahedron, from which it deviates significantly.

VI. The Degree of Icosahedricity of Distorted C_{60}-Fullerene Anions. In all previous examples, both model and real, the number of vertexes of the perfect polyhedron was the minimal to support the polyhedricity. However, the tool we developed here is capable in fact of dealing with *any* number of vertexes that can support a given polyhedricity. Thus, whereas above we looked at a 12-vertex icosahedron, we shall now analyze a 60-vertex distorted icosahedron. We selected this example because of the substantial interest in the structural changes that the perfect icosahedral C_{60} fullerene undergoes upon substitution, ionization, and intracage entrapment.[19] Many of the properties of this molecule are intimately related to its high, perfect symmetry and therefore also to distortions from it. The example we have chosen is the study of Green et al.[20] on the electronic structures of a series of C_{60} anions. Green et al. found that the perfect icosahedricity of the fullerene is distorted upon extra charging of this molecule and that the degree of this JT-induced distortion changes with amount of charge. An excellent correlation between the degree of icosahedricity and charge was obtained (Figure 5). It is significant that bond lengths and the norm distortion vectors (Table 1 in ref 20) do not follow the increase in charge, whereas the symmetry measure does; a global descriptor, symmetry, works here much better than a specific, local one. A detailed analysis

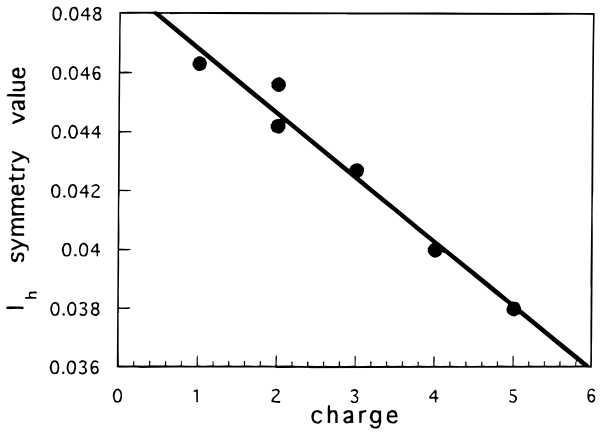

Figure 5. C_{60}-fullerene anions undergo Jahn−Teller distortion of the original prefect icosahedral structure of the neutral molecule.[20] Shown is the correlation between the degree of icosahedricity of C_{60}-fullerene anions and their charge. (For the distorted dianion: upper point, singlet; lower, triplet.)

of the unique correlation of Figure 5, made possible in fact only by treating symmetry as a measurable quantity, and of other correlations that emerge from ref 20 will be the topic of a separate report, due to the special importance of this molecule.

5. Conclusion

We have extended the continuous symmetry measures approach to polyhedra. The methodology and the general computational tool we developed are general and applicable to the assessment of the minimal distance of a structure to any desired shape. Specifically, we demonstrated the polyhedricity measure for the quantitative evaluation of the symmetry of the most abundant polyhedral structures, both on models and on real examples. The correlation found for the fullerene case (Figure 5) points to the direction of our future activity in this field; once the degree of polyhedricity can be measured, how do the various properties of polyhedral complexes, clusters, and covalent structures correlate quantitatively with symmetry? We have already reported on three other cases where symmetry as a global structural parameter correlates better with physical/chemical properties than specific descriptors. One case has been the relation between the degree of chirality of enzymatic inhibitors and their inhibition efficiency,[21] a second case related the symmetry-normalized energy of isomerization of chiral fullerenes to their size,[22] and a third case identified the melting point of deuterium clusters.[4a] In fact, these correlations along with the new one shown in Figure 5 strengthen our belief that the specific symmetry measurement tool we designed reflects the physical world properly.

Acknowledgment. We thank Prof. P. Fowler for providing us the coordinates of the anion-fullerenes.

Appendix A: The Minimizations

a. Minimization with Respect to the Translation Vector T. Differentiating eq 4 with respect to the vector **T** and setting the derivative equal to zero yields

(19) Fowler, P. W.; Ceulemans, A. *J. Phys. Chem*. **1995**, *99*, 508.
(20) Green, W. H., Jr.; Gorun, S. M.; Fitzgerald, G.; Fowler, P. W.; Ceulemans, A.; Titeca, B. C. *J. Phys. Chem*. **1996**, *100*, 14892.
(21) Keinan, S.; Avnir, D. *J. Am Chem. Soc*. **1998**, *120*, 6152.
(22) Pinto, Y.; Fowler, P. W.; Mitchell, D.; Avnir, D. *J. Phys. Chem*. **1998**, *102*, 5776.

$$\sum_{i=1}^{N} [Q_i - (A\mathbf{R}P_{0i} + \mathbf{T})] = 0 \quad \text{(A1)}$$

Since we chose to place both centers of mass (of the original and of the general shape, prototype polyhedrons) at the origin of coordinates, this equation gives $\mathbf{T} = 0$. Consequently, the centers of mass of the nonsymmetric polyhedron and the nearest perfect polyhedron coincide as well. In what follows, we use therefore $\mathbf{T} = 0$ and minimize the function

$$J = \sum_{i=1}^{N} |Q_i - A\mathbf{R}P_{0i}|^2 = \sum_{i=1}^{N} |Q_i|^2 - 2A\sum_{i=1}^{N} P_{0i}^{t}\mathbf{R}^{t}Q_i + A^2\sum_{i=1}^{N} |\mathbf{R}P_{0i}|^2 \quad \text{(A2)}$$

In (A2) the upper index t shows the transposition of the matrix or vector. As rotation does not affect the distance between the center of mass and vertexes, the last term in (A2) can be taken as

$$A^2\sum_{i=1}^{N} |\mathbf{R}P_{0i}|^2 = A^2\sum_{i=1}^{N} |P_{0i}|^2 = NA^2$$

Hence, eq A2 can be written as

$$J = \sum_{i=1}^{N} |Q_i - A\mathbf{R}P_{0i}|^2 = \sum_{i=1}^{N} |Q_i|^2 - 2A\sum_{i=1}^{N} P_{0i}^{t}\mathbf{R}^{t}Q_i + NA^2 \quad \text{(A2′)}$$

b. Minimization with Respect to the Scaling Factor *A*. Differentiating (A2′) with respect to A and setting the derivative equal to zero, we derive the equation for the scaling factor,

$$A = \frac{1}{N}\sum_{i=1}^{N} P_{0i}^{t}\mathbf{R}^{t}Q_i \quad \text{(A3)}$$

c. Minimization with Respect to Rotation Angles. The rotation matrix $\mathbf{R}$ can be determined using three rotation angles α, β, γ. By differentiation of (A2′) with respect to Eulerian angles and setting the derivatives equal to zero, the following equations for rotations angles are derived.

$$\sum_{i=1}^{N} P_{0i}^{t}\frac{\partial \mathbf{R}^{t}}{\partial \alpha}Q_i = \sum_{i=1}^{N} P_{0i}^{t}\frac{\partial \mathbf{R}^{t}}{\partial \beta}Q_i = \sum_{i=1}^{N} P_{0i}^{t}\frac{\partial \mathbf{R}^{t}}{\partial \gamma}Q_i = 0 \quad \text{(A4)}$$

It is essential to point out that the solutions to eq A4, are independent of the scaling factor, A. Therefore, eqs A3 and A4 can be solved independently. Thus, one can first solve eq A4 and then use the data to calculate the scaling factor A from eq A3. As a rule, eq A4 cannot be solved analytically. To solve it methods described in refs 23 and 24 can be used. Substituting (A1) and (A3) into (1) and taking into account the fact that the center of mass of an asymmetric polyhedron is located at the origin of coordinates (i.e., $Q_0 = 0$), we arrive at eq 5.

Appendix B: Probability Theory Interpretation of the Symmetry Measure

It is interesting to note that eq 5 can be interpreted in terms of probability theory. Let us assume Q_k to be a random set of points coordinates with zero average, i.e., with $Q_0 = 0$. Using this random set, we obtain the nearest symmetric polyhedron to it (in the statistical sense). To see that this is indeed possible, let us rewrite (5) as

$$S = \left\{1 - \left[\frac{\frac{1}{N}\sum_{k=1}^{N} P_{0k}^{t}\mathbf{R}^{t}Q_k}{\left(\frac{1}{N}\sum_{k=1}^{N}\left|P_{0k}^{t}\right|^2\right)^{1/2}\left(\frac{1}{N}\sum_{k=1}^{N}\left|\mathbf{R}^{t}Q_k\right|^2\right)^{1/2}}\right]^2\right\} \times 100 = \left\{1 - \left[\frac{\frac{1}{N}\sum_{k=1}^{N} \hat{P}_{k}^{t}Q_k}{\left(\frac{1}{N}\sum_{k=1}^{N}\left|\hat{P}_k\right|^2\right)^{1/2}\left(\frac{1}{N}\sum_{k=1}^{N}\left|Q_k\right|^2\right)^{1/2}}\right]^2\right\} \times 100$$

The expression in the square brackets is in fact a sampling correlation coefficient, ρ, between the original random coordinates and the vertex coordinates of the nearest symmetric polyhedron. Thus, it is possible to connect the continuous symmetry measure S with the correlation coefficient ρ:

$$S = (1 - \rho^2) \times 100 \quad \text{(5′)}$$

Appendix C: The Limiting $S(O_h)$ Values of a Perfect Octahedron Undergoing *z*-Axis Distortions

For extreme elongation of the octahedron along the z-axis, the distance Q between the two vertexes on the Z-axis and center of mass is much larger than the distances of the other vertexes. Using eq 5, one obtains then

$$S = \left[1 - \frac{(\sum_{k=1}^{6} P_{0k}^{t}\mathbf{R}^{t}Q_k)^2}{6\sum_{k=1}^{6}|Q_k|^2}\right] \times 100 = \left[1 - \frac{(2Q)^2}{6(2Q^2)}\right] \times 100 = \frac{2}{3} \times 100$$

For extreme compression, the situation reverses; the distance of the two z-axis vertexes to the center of mass approaches zero, and one must take into account only the four other distances. From eq 5

$$S = \left[1 - \frac{(\sum_{k=1}^{6} P_{0k}^{t}\mathbf{R}^{t}Q_k)^2}{6\sum_{k=1}^{6}|Q_k|^2}\right] \times 100 = \left[1 - \frac{(4Q)^2}{6(4Q^2)}\right] \times 100 = \frac{1}{3} \times 100$$

These two limits are clearly seen in Figure 3.

IC9804925

(23) Arun, K. S.; Huang, T. S.; Blostein, S. D. *IEEE Trans. Pattern Anal. Machine Intel.* **1987**, *PAMI-9*, 698.
(24) Horn, B. K. P. *J. Opt. Soc. Am.* **1987**, *A4*, 629.